Amino Acid 305 Determines Catalytic Center Accessibility in CYP3A4†

Stephen M. Fowler,*,‡ Robert J. Riley,§ Michael P. Pritchard,‡ Michael J. Sutcliffe,|| Thomas Friedberg,‡ and C. Roland Wolf‡

Biomedical Research Centre, Ninewells Hospital and Medical School, Dundee DD1 9SY, U.K., Department of Physical and Metabolic Sciences, AstraZeneca R&D Charnwood, Bakewell Road, Loughborough LE11 5RH, U.K., and Department of Chemistry, University of Leicester, Leicester LE1 7RH, U.K.

Received October 12, 1999; Revised Manuscript Received January 13, 2000

ABSTRACT: Site-directed mutagenesis has been used to replace alanine 305 with phenylalanine (A305F) and serine (A305S) in the active site of cytochrome P450 3A4 (CYP3A4). Enzyme kinetics for diazepam, erythromycin, nifedipine, and testosterone metabolism have been determined for both mutants and wild-type CYP3A4. The A305F mutation abolished diazepam oxidase activity and reduced the S_{50} and V_{max} for erythromycin *N*-demethylase activity from 17 to 10 μM and from 3.2 to 1.2 pmol product/min/pmol P450, respectively. The V_{max} for testosterone 6β-hydroxylase activity was also significantly reduced, from 2.3 to 0.6 pmol product/min/pmol P450, whereas the S_{50} increased from 33 to 125 μM. The nifedipine oxidase activity was diminished to a lesser extent, down from 6.5 to 4.9 pmol product/min/pmol P450, whereas the S_{50} increased from 9 to 42 μM. The K_i for ketoconazole, a CYP3A4 selective inhibitor, was increased more than 10-fold from 0.050 to 0.55 μM, from 0.052 to 0.73 μM, and from 0.043 to 2.2 μM by the A305F mutation when measured against erythromycin, nifedipine, and testosterone metabolism activities, respectively. Similarly, the inhibition constants of the broader specificity inhibitors; clotrimazole, econazole, and miconazole were increased 3- to 15-fold by the A305F mutation. In contrast, the A305S mutation increased testosterone 6β-hydroxylase (V_{max} = 2.9 pmol product/min/pmol P450) and erythromycin *N*-demethylase (V_{max} = 5.1 pmol product/min/pmol P450) activities, but reduced nifedipine oxidase activity (V_{max} = 4.6 pmol product/min/pmol P450). K_i values for ketoconazole and other azole inhibitors were unchanged by the A305S mutation. It is proposed that in CYP3A4, the mutagenesis of alanine 305 to a phenylalanine increases the steric hindrance of the catalytic center, thereby greatly reducing azole inhibitor binding affinity, but maintaining monoogygenase activity.

The cytochromes P450 are a class of heme-thiolate enzymes that catalyze the regio- and stereoselective oxidation of a wide variety of xenobiotic and pharmaceutical compounds. Cytochrome P450 3A4 (CYP3A4)[1] is the most abundant human liver cytochrome P450 isoform. It catalyzes the oxidation of a multitude of important drugs, ranging from the anaesthetic lidocaine, antibiotics such as erythromycin, the cancer chemotherapeutics Taxol and ifosphamide, to steroids such as testosterone and progesterone (*1*, *2*). In the absence of a crystal structure for CYP3A4, or any other mammalian cytochrome P450, homology modeling and site-directed mutagenesis approaches have been adopted for the investigation of enzyme−substrate interactions. To date, such studies have concentrated upon the ability of the extensive CYP3A4 active site to accommodate more than one substrate molecule simultaneously and the resultant activation/enhancer effects. Amino acid residues in at least four different regions of the primary sequence have been identified as contributing to the enhancer effects exhibited by α-naphthoflavone, with some concomitant alterations in steroid hydroxylase regioselectivity also reported (*3*−*5*).

The I-helix is a major structural element conserved throughout cytochromes P450 that runs through the core of the enzyme, incorporating amino acids involved in heme coordination and substrate binding and playing an essential role in the oxidation reaction process (*6*).

Two regions of the I-helix have been shown to be important for the activity of cytochromes P450. First, a region of helix distortion associated with a *Gx(E/D)T* motif has been found in all of the cytochromes P450 (*7*). Detailed studies in CYP101 ($P450_{cam}$) and CYP102 ($P450_{BM-3}$) have shown that an acidic side chain adjacent to a threonine form a critical part of the hydrogen-bonding network that facilitated dioxygen scission (*8*−*10*). For the mutagenesis studies in which either of these residues was altered, even with highly conservative mutations, such as glutamic acid to aspartic acid or threonine to serine, enzyme efficiency was attenuated (*9*, *11*, *12*). In CYP3A4, the corresponding amino acids are

† The authors thank the following sources for funding of this work: Wellcome Trust, Grant No. 041641/Z/94/Z (S.M.F.); ICRF/MRC Programme Grant G920317S (C.R.W., M.J.S.); BBSRC/DTI/Pharmaceutical industry funding (M.P.P., T.F.).

* Corresponding Author. Current Address: Department Physical and Metabolic Sciences, AstraZeneca R&D Charnwood, Bakewell Road, Loughborough LE11 5RH, U.K. Tel: (44)-1509-644225. Fax: (44)-1509-645557. E-mail: stephen.fowler@astrazeneca.com.

‡ Ninewells Hospital and Medical School.

§ AstraZeneca R&D Charnwood.

|| University of Leicester.

[1] Abbreviations used: CHAPS, (3-(3-cholamidopropyl)dimethylammonion-1-propane) sulfonate; CYP, Cytochrome P450; DMSO, dimethylsulfoxide; IPTG, isopropylthio-D-β-galactopyranoside; NADPH, β-nicotinamide adenine dinucleotide, reduced form; SDS−PAGE, sodium dodecyl sulfate − polyacrylamide gel electrophorsis.

10.1021/bi992372u CCC: $19.00 © 2000 American Chemical Society
Published on Web 03/24/2000

glutamic acid 308 and threonine 309. Second, in CYP2D6, aspartic acid 301 has the potential to form a charge interaction that would assist in the binding of basic substrates. This interaction localizes the positively charged part of a substrate molecule within the active site, directing oxidation to a position typically 5−7 Å from the basic center (*13*, *14*). The replacement of aspartic acid 301 with a glutamic acid resulted in the reduction of debrisoquine hydroxylase activity, and it altered metoprolol oxidation regioselectivity. The removal of the acidic function resulted in an almost complete loss of CYP2D6 activity (*15*).

Alanine 305 is located between these two regions of the I-helix in CYP3A4. Our molecular modeling studies, and those of Szklarz and Halpert (*16*), predicted alanine 305 to be located close to the catalytic center with the potential to make some contacts with bound substrate molecules. The mutagenesis of alanine 305, therefore, raised the intriguing possibility of using the I-helix as a relatively rigid scaffold upon which to build new enzyme functionalities, by site-directed mutagenesis. In this study, site-directed mutants of CYP3A4 have been constructed in which alanine 305 has been replaced with either a phenylalanine residue (A305F) or a serine residue (A305S). These mutations alter the character of the amino acid 305 side chain from a small hydrophobic moiety to one with the potential for forming new hydrophobic bonding interactions (A305F) or one in which enzyme−substrate hydrogen bonds may be introduced (A305S).

Compounds containing azole or pyridine moieties have been found to be potent inhibitors of cytochromes P450 (*17*−*19*). Although competitive inhibition has been examined between substrates, such as testosterone and erythromycin, the active-site features which favor enzyme inhibition by the most potent class of CYP3A4 inhibitors—azole containing hydrophobic compounds—have not been examined. The ability of a compound to act as a ligand and form a direct bonding interaction with the heme iron, in addition to making charge or hydrophobic binding interactions within the active site, is likely to increase the strength of ligand binding. Clotrimazole, miconazole, and ketoconazole are all highly potent competitive inhibitors of CYP3A4. Of these compounds, ketoconazole is commonly used as a selective CYP3A4 inhibitor in the presence of other human CYP isoforms (*20*), but the structural features of the inhibitor that underlie the CYP3A4 selectivity are not clearly understood.

In this study, the effects of the A305F and A305S mutations on a wide variety of prototypical CYP3A4 substrates, including a steroid (testosterone), a dihydropyridine (nifedipine), a benzodiazepine (diazepam), and a macrolide antibiotic (erythromycin) have been examined. The inhibition potencies (K_i values) of four potent and three weak azole-containing inhibitors have also been determined. The variety of substrate and inhibitor structures investigated has enabled the general, as well as substrate/inhibitor specific, effects of alanine 305 substitution to be assessed.

METHODS

All of the reagents and fine chemicals were obtained from Sigma−Aldrich (Poole, Dorset) with the following exceptions: IPTG, GibcoBRL/Life Technologies; aprotinin, ampicillin, and leupeptin, Boehringer Mannheim; *N*-methyl[^{14}C]-erythromycin, NEN Life Products. Enzymes for DNA manipulation were obtained from Promega.

Expression of CYP3A4 and Cytochrome P450 Reductase in Escherichia coli. Expression experiments were carried out, as described in Blake et al. (*21*) and Pritchard et al. (*22*,*23*), using the expression vectors pB35 and pB212. *E. coli* membranes containing CYP3A4 and human cytochrome P450 reductase were prepared by the method of Blake et al. (*21*) and resuspended in detergent-free 1× TSE buffer (50 mM Tris Acetate, pH 7.6, 250 mM sucrose, 0.25 mM EDTA). The cytochrome *c* (horse heart, Sigma) reductase activity was determined spectroscopically by the method of Vermilion and Coon (*24*), monitoring at 550 nm, with an extinction coefficient change of 21 400 M^{-1} cm^{-1}. This indicated P450 reductase concentrations to be greater than 3× that of CYP3A4. All of the experiments were carried out in the absence of Cytochrome b_5. Mutagenesis reactions were performed following the single-stranded method of Kunkel (*25*). The reverse complementary primers 5′-CGTG-GTTTCATAGCCAAAAAAAATAAAGATAAT-3′ and 5′-CGTGGTTTCATAGCCAGAAAAAATAAAGATAAT-3′ introduced the A305F and A305S mutations, respectively. Transformant clones were checked for mutagenesis by manual dideoxy chain termination sequencing using the T7 Sequenase kit (Amersham).

Modification of the pB35-A305F Plasmid to Incorporate a C-Terminal Hexa-Histidine Coding Sequence. Protein generated from the CYP3A4 expression plasmid pB83 (derived from pB35, in which the 3′ end of the cDNA sequence had been modified to encode a protein whose C-terminus included and hexa-histidine sequence) was used for spectroscopic studies of wild-type CYP3A4. To generate the equivalent A305F construct, the plasmids pB35-A305F and pB83 were digested with *Sca*I, and the resulting fragments were purified from an agarose gel. Ligation of the minor pB83 *Sca*I fragment to the major pB35-A305F fragment generated the histidine tagged form of A305F (pB83-A305F). The transformant clones were screened to ensure the correct insert orientation by plasmid preparation followed by *Hin*dIII restriction digest and agarose gel electrophoresis. Enzyme solubilization and purification were carried out as described by Pritchard et al (*22*) using a HiTrap nickel−agarose chelating column (Pharmacia).

Diazepam, Nifedipine, and Testosterone Oxidation. Metabolism Kinetics. Substrate and inhibitor stock solutions were made up at 100× the final reaction concentration in DMSO. Two microliters of substrate stock was added to each reaction tube, followed by 178 μL of *E. coli* membrane solution. (The final incubation components were 50 mM potassium HEPES, 20 mM magnesium chloride, pH 7.4, 1% v/v DMSO, 35 pmol P450, and total volume 200 μL.) The assay mixtures were preincubated for 3 min at 37 °C in a thermostated heater block, and the reaction was started by the addition of 20 μL of 10 mM NADPH (freshly dissolved in water and stored on ice). The reactions were quenched after 3−5 min at 37 °C (5 min for diazepam, 4 min for testosterone, and 3 min for nifedipine) by the addition of 25 μL of 10% w/v trichloroacetic acid followed by 50 μL of methanol. Quenched reactions were mixed by inversion and chilled to −20 °C for at least 1 h to maximize the protein precipitation. Following centrifugation (15 min, 3500 rpm, IEC Centra8R benchtop centrifuge), 150 μL of supernatant

Table 1: High-Pressure Liquid Chromatography Conditions Used for Analysis of Diazepam, Nifedipine, and Testosterone Metabolism

substrate	mobile phases	flow rate (mL/min)	detection wavelength (nm)	mobile phase profiles: timepoint (min)	mobile phase profiles: % solvent A	substrate/ metabolite	elution time (min)
diazepam	A: acetonitrile	1.5	257	0	27	oxazepam	4.0
	B: 0.25% w/v ammonium acetate			4	27	temazepam	5.5
				7	65	nordiazepam	6.2
				8.5	50	diazepam	7.8
nifedipine	A: acetonitrile	1.5	218	0	30	oxidized nifedipine	4.9
	B: 0.025% w/v ammonium acetate			2	30	nifedipine	6.1
				5	40		
				5.5	50		
				6	95		
				6.5	95		
testosterone	A: 95% acetonitrile, 5% methanol	1.5	254	0	15	6β-hydroxytestosterone	5.4
				12	72	15β-hydroxytestosterone	7.4
	B: 95% (0.025% w/v ammonium acetate), 5% methanol			15	80	2β-hydroxytestosterone	8.8
						testosterone	13.9

was transferred to HP1100 HPLC vials for analysis.

Ketoconazole Inhibition. Enzyme assays were performed at substrate concentrations equal to the S_{50} value determined for each enzyme form. A178 μL portion of *E. coli* membranes/substrate was added to 2 μL of inhibitor. The enzyme activities were then determined, as above, in the presence of 0.01 to 10 μM ketoconazole.

Erythromycin N-Demethylase Activity Determinations. The release of ^{14}C-radiolabeled formaldehyde was used to determine erythromycin *N*-demethylase activity. In each assay, the concentration of labeled erythromycin was maintained at 10 μM, whereas the concentration of cold erythromycin was varied between 0 and 590 μM. The incubations were carried out as for nifedipine and testosterone, with the exception that the labeled erythromycin was added to the *E. coli* membrane solution at the outset. The reaction components were 103 μL of *E. coli* membranes/labeled erythromycin, 2 μL of cold erythromycin (100× stock solutions in DMSO), and 75 μL of water. A 6 min incubation at 37 °C followed the preincubation and the reaction initiation. The reactions were quenched by the addition of 25 μL of 10% w/v trichloroacetic acid, and a solid-phase extraction was carried out on the entire reaction mix, as described by Moody et al (*26*). Liquid scintillation counting was used to determine the amount of labeled formaldehyde released, with the turnover rate calibrated against the radioactivity of a known concentration of erythromycin corrected for background radioactivity. The total activities were then calculated, based upon the relative abundance of labeled and cold erythromycin in each reaction.

Inhibition experiments were carried out by the method of Moody et al (*26*), with the exception that an erythromycin concentration of 10 μM, 20 pmol P450/reaction, and an incubation time of 6 min were used. Azole inhibitor concentrations between 0.01 and 10 μM were tested for ketoconazole, econazole, miconazole, and clotrimazole, whereas concentrations of 0.05 to 50 μM were used for the other, less potent, inhibitors.

Spectroscopic Observation of Azole Binding. Samples of purified, histidine-tagged CYP3A4 and CYP3A4-A305F were desalted, and the imidazole was removed by passage through a 10 mL Sephadex P10 gel filtration column (Pharmacia) preequilibrated with spectroscopy buffer (100 mM potassium phosphate (pH 7.5), 0.1% w/v CHAPS, 20% v/v glycerol, and 0.1 mM dithiothreitol). The resultant enzyme samples were found to be >90% homogeneous when analyzed by SDS−PAGE and gave absolute spectra with a Soret maximum at 418 nm. Difference spectroscopy was performed using a Shimadzu UV3000 spectrophotometer; identical enzyme samples were added to matched sample and reference cuvettes, and the baseline was set. Equal volumes of azole compound solution and pure solvent (DMSO) were added to the sample and the reference cuvettes, respectively, and the difference spectra were recorded between 500 and 360 nm.

Analytical Methods. All analyses were carried out using reversed-phase high-pressure liquid chromatography, the conditions of which are shown in Table 1. A Hewlett-Packard HP1100 system, equipped with binary pump, column thermostat, variable-wavelength detector, and Waters symmetry shield RP_8 (3.9 × 50 mm) analytical cartridge, was used throughout. The product generation was calibrated against commercially available authentic standards.

Data Treatment. A nonlinear regression analysis was performed using the program WinNonlin (Standard Edition, Version 1.1, Scientific Consulting, Inc.) with either a Michaelis−Menten or a Hill plot fitted to the substrate saturation data, as appropriate to the enzyme/substrate combination. A simple inhibition effect model was fitted to the inhibition data. K_i values were calculated using the relationship $K_i = IC_{50}/(S_{50} + [S])$, where [S] was the substrate concentration used in the assay, S_{50} was the half-saturation substrate concentration and IC_{50} was the inhibitor concentration required for half inhibition of enzyme activity.

RESULTS

Enzyme Activities. Both the wild type and the A305F mutant exhibited sigmoidal kinetics for testosterone metabolism (Figure 1) and Michaelis−Menten hyperbolic kinetics for erythromycin *N*-demethylase (Figure 2) and nifedipine oxidase (Figure 3) activities. The A305S mutant showed

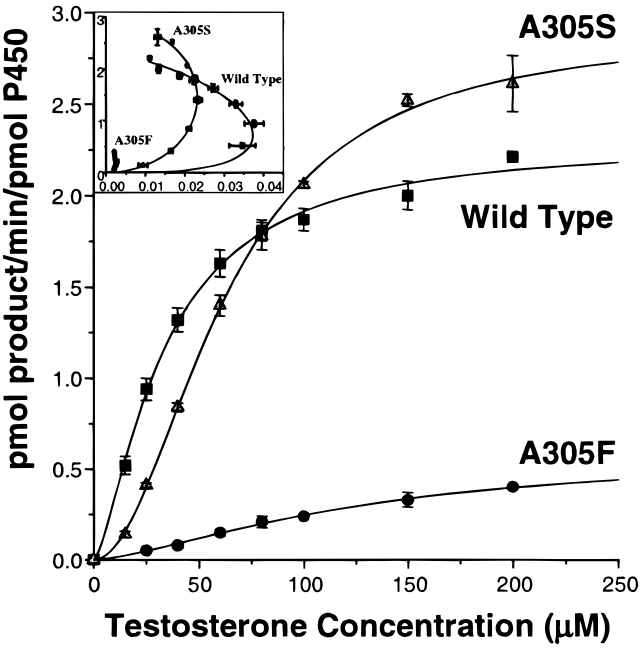

FIGURE 1: Testosterone 6β-hydroxylase kinetics. Plot of reaction rate (pmol product/min/pmol P450) against substrate concentration (μM) for CYP3A4 wild type (filled squares), A305F (filled circles), and A305S (filled triangles). Values plotted are average of three determinations, with error bars showing one standard deviation. Comparable Eadie−Hoftsee plot inset (reaction rate plotted against reaction rate/testosterone concentration for the same data).

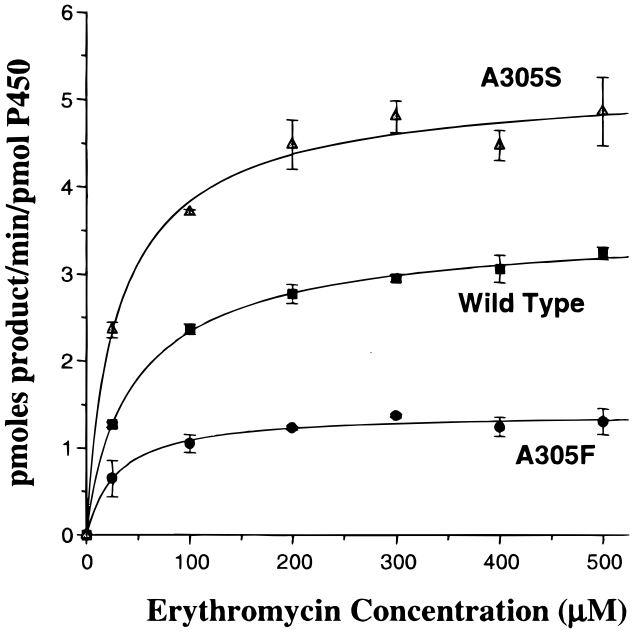

FIGURE 2: Erythromycin *N*-demethylase kinetics. Plot of reaction rate (pmol product/min/pmol P450) against substrate concentration (μM) for CYP3A4 wild type (filled squares), A305F (filled circles), and A305S (filled triangles). Values plotted are average of three determinations, with error bars showing one standard deviation.

sigmoidal kinetics for diazepam (Figure 4), nifedipine, and testosterone metabolism but Michaelis−Menten hyperbolic kinetics for erythromycin *N*-demethylase activity. The mutation of alanine 305 did not, therefore, alter the active site such as to prevent the simultaneous binding of the two testosterone/diazepam molecules required for allosteric autoactivation (Figures 1 and 4), nor did it alter the character of the erythromycin *N*-demethylase kinetics.

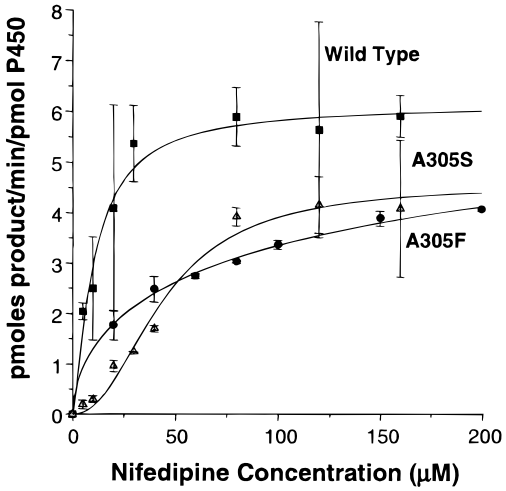

FIGURE 3: Nifedipine oxidase kinetics. Plot of reaction rate (pmol product/min/pmol P450) against substrate concentration (μM) for CYP3A4 wild type (filled squares), A305F (filled circles), and A305S (filled triangles). Values plotted are average of three determinations, with error bars showing one standard deviation.

The A305F mutation reduced the activity of CYP3A4 toward all of the substrates investigated. However, the magnitude of this effect was strongly substrate dependent. For example, the V_{max} values for nifedipine oxidase and erythromycin *N*-demethylase activities were 75% and 37% of those of the wild type, respectively, whereas maximum testosterone 6β-hydroxylase activity was only 26% of the wild type, and diazepam metabolism was not detectable at all (Table 2). The activities of the A305S mutant were generally higher than those of the wild type, by 26% for testosterone 6β-hydroxylase, 20% for diazepam *N*-demethylase, and 57% for erythromycin *N*-demethylase. Conversely, maximal nifedipine oxidase and diazepam 3-hydroxylase activities were 29% and 38% lower than those of the wild type, respectively. These activity differences were less striking than those caused by the A305F mutation.

Enzyme Regioselectivity. In CYP3A4, the A305S mutation reduced the regioselectivity of diazepam oxidation, relative to the wild type (Table 3), although it slightly increased the regioselectivity of the testosterone hydroxylase activity. Testosterone hydroxylase regioselectivity appeared unchanged for the A305F mutant, although the total quantity of the hydroxylated products generated was too low to allow 15β-hydroxytestosterone quantitation. This retention of testosterone hydroxylase regioselectivity suggested that neither mutation significantly altered the preferred orientation of the testosterone's approach to the catalytic center. In contrast, the A305F mutation abolished diazepam oxidase activity completely, and the A305S mutation reduced the CYP3A4 diazepam 3-hydroxylase/*N*-demethylase ratio from 7 to 3. Thus, the active-site region close to amino acid 305 clearly made an important contribution to diazepam binding and metabolism, whereas the retention of CYP3A4 testosterone hydroxylase regioselectivity suggested that testosterone interacted little with this residue in the active site.

Reduction of Ketoconazole Inhibition Potency by the A305F Mutation. The inhibition of testosterone 6β-hydroxylase activity for the wild type, A305F, and A305S forms of CYP3A4, carried out with substrate concentration equal to the S_{50} for each enzyme, is shown in Figure 5. The K_i values

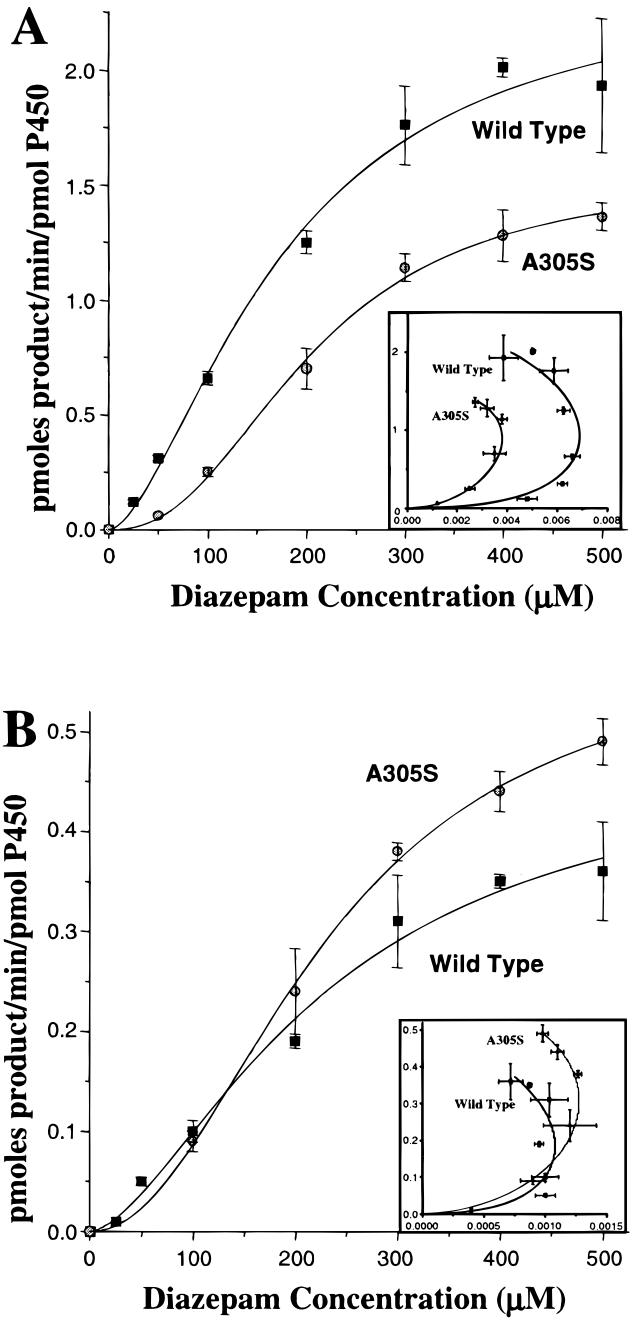

FIGURE 4: Diazepam oxidation kinetics. Plots of (A) diazepam 3-hydroxylase and (B) diazepam *N*-demethylase reaction rates (pmol product/min/pmol P450) against substrate concentration (μM) for CYP3A4 wild type (filled squares) and A305S (filled circles). Values plotted are average of three determinations, with error bars showing one standard deviation. Comparable Eadie−Hoftsee plots inset (reaction rate plotted against reaction rate/diazepam concentration for the same data).

for ketoconazole inhibition of testosterone 6β-hydroxylase activity were 0.043, 2.2, and 0.021 μM for the wild type, A305F, and A305S, respectively (Table 4). The inhibition profile for the A305S mutant was almost identical to the wild type, whereas the testosterone hydroxylase activity of the A305F mutant was 50-fold less sensitive to ketoconazole inhibition. To eliminate the possibility of substrate-specific effects, ketoconazole inhibition potency was also determined using a further two assays, erythromycin *N*-demethylase and nifedipine oxidase activities. Here, K_i values for the A305F mutant were found to be 11-fold and 15-fold higher than those of the wild type, respectively (Table 4). The inhibition constants of the A305S mutant were close to wild-type values in all three determinations.

Reduction of Azole Compound Inhibition Potency. To determine whether the A305F mutation had resulted in an effect specific to ketoconazole, or whether reduction in ketoconazole inhibition potency was a specific example of a more general effect, the inhibition properties of a range of azole-containing compounds were determine using the sensitive erythromycin *N*-demethylase assay (Table 5). The compounds tested included the high-affinity CYP3A4 inhibitors; clotrimazole, miconazole, and econazole; and three lower affinity 1-phenylimidazole derivatives (structures shown in Figure 6). The K_i values that were obtained using the wild-type CYP3A4 and the A305S mutant were similar for all of these inhibitors, whereas those of the A305F mutant were between 3- and 16-fold higher.

Spectroscopic Observation of Ketoconazole and Imidazole Binding. The effect of the A305F mutation on azole compound binding has also been observed directly. The spectroscopic characteristics of cytochrome P450 enzymes with a variety of distal ligands are well established (*27*). On the displacement of water and the binding of an aromatic nitrogen ligand, such as an azole or pyridine, a shift in the Soret absorption band is seen from $\lambda_{max} = 418$ to 422 nm. The proportion of enzyme that had taken up the new heme ligand could be determined using difference spectroscopy (Figure 7). Figure 8 shows the ligand saturation profiles of the wild-type CYP3A4 and the A305F mutant, using ketoconazole and imidazole as ligands. To achieve half-saturation, the A305F mutant required a concentration of ketoconazole of at least 10-fold higher than that required to half-saturate the wild-type enzyme. Even imidazole, the smallest possible azole ligand, required a 3-fold greater concentration ($\sim$1.3 vs $\sim$0.5 mM) to half-saturate the A305F mutant than the wild-type CYP3A4. These spectroscopic observations provided direct evidence that the reduced sensitivity of the A305F mutant to ketoconazole inhibition was associated with reduced heme binding affinity of the azole moiety.

The absolute concentration of ligand required for enzyme saturation was noticeably higher in the spectroscopic assay than observed in the metabolism assays. This could have been due to the amount of enzyme required to obtain clear difference spectroscopy traces ($\sim$0.5 μM), which set the lower limit for the dissociation constant determination to $>$0.5 μM. In addition, the presence of 0.1% w/v CHAPS may have altered the partitioning between the aqueous solution and the enzyme active site.

DISCUSSION

Metabolic Activities. The investigations of Domanski et al. (*3*) have shown that, on mutation of alanine 305 to a glycine (A305G) or valine (A305V), the wild-type CYP3A4 activities were generally maintained. The testosterone hydroxylase activity of the mutant enzymes was reduced by up to 40%, and a shift in the regioselectivity of testosterone hydroxylation was also observed, with the A305G mutant showing reduced 6β-hydroxylase specificity, principally in favor of increased 2β-hydroxylase activity. Similarly, both the A305G and the A305V mutants showed reduced proges-

Table 2: Oxidation Kinetics for Prototypical CYP3A4 Substrates[a]

CYP3A4 enzyme	testosterone 6β-hydroxylase		diazepam 3-hydroxylase		diazepam *N*-demethylase		erythromycin *N*-demethylase		nifedipine oxidase	
	S_{50}	V_{max}	S_{50}	V_{max}	S_{50}	V_{max}	S_{50}	V_{max}	S_{50}	V_{max}
wild type	33 ± 2	2.3 ± 0.1	176 ± 33	2.4 ± 0.3	217 ± 52	0.5 ± 0.1	17 ± 1	3.2 ± 0.1	9 ± 4	6.5 ± 0.5
A305F	125 ± 31	0.6 ± 0.1	ND	ND	ND	ND	10 ± 2	1.2 ± 0.1	42 ± 8	4.9 ± 0.3
A305S	63 ± 2	2.9 ± 0.1	208 ± 18	1.5 ± 0.1	236 ± 27	0.6 ± 0.1	29 ± 3	5.1 ± 0.1	45 ± 8	4.6 ± 0.5

[a] In this table, S_{50} values quoted are in μM, and V_{max} values are in pmol product/min/pmol P450. ND: not detected, no diazepam metabolism detected for the A305F mutant. Detection limits: 3-hydroxylase activity 0.02 pmol product/min/pmol P450; *N*-demethylase activity 0.03 pmol product/min/pmol P450.

Table 3: Regioselectivity of Testosterone and Diazepam Oxidation Reactions. Activities Measured at Substrate Concentrations of 200 μM[a]

CYP3A4 form	testosterone hydroxylase activity			diazepam	
	6β	15β	2β	3-hydroxylase	*N*-demethylase
wild type	87 ± 1	4 ± 1	9 ± 1	87 ± 1	13 ± 1
A305F	90 ± 9	ND	10 ± 1	ND	ND
A305S	92 ± 1	1 ± 1	7 ± 1	75 ± 1	25 ± 1

[a] ND: not detected.

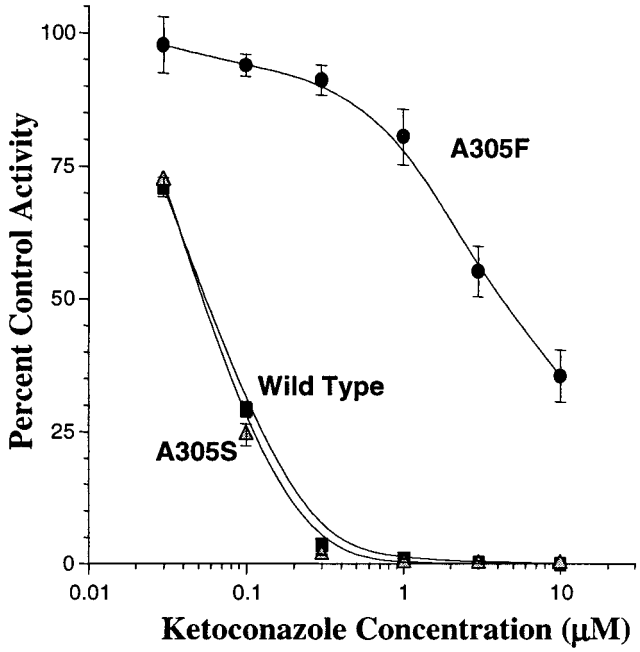

FIGURE 5: Ketoconazole inhibition of testosterone 6β-hydroxylase activity. Percent control activity (no ketoconazole control activity set to 100%) plotted against ketoconazole concentration (μM) for wild-type CYP3A4 (filled squares), A305F (filled circles), and A305S (filled triangles). Average of three determinations and one standard deviation shown.

terone hydroxylase activities, relative to the wild type, with 16α-hydroxylase activity affected to a greater extent than 6β-hydroxylase activity by the A305V mutation. The A305V substitution also modified the behavior of α-naphthoflavone, thus reducing steroid hydroxylase activity enhancement and increasing the degree of competitive inhibition.

This study builds upon the findings of Domanski et al. (*3*) and has characterized the effects of alanine 305 mutagenesis in detail. The kinetics of diazepam, erythromycin, nifedipine, and testosterone oxidation reactions, which represent a wide variety of CYP3A4 activities, have been presented. It was found that half-saturation concentrations for testosterone, diazepam, and nifedipine metabolism reactions were all increased on mutation of alanine 305. The substrate saturation profiles (Figures 1, 3, and 4) illustrate that, for the two mutants, this was the result of quite different effects. The A305F mutant appeared to have a lower affinity for testosterone and nifedipine, resulting in saturation profiles equivalent to the wild-type enzyme but shifted toward lower turnover and higher substrate concentration. The A305S mutant demonstrated enhanced autoactivation characteristics (Figures 1 and 4) such that the main cause of the increased S_{50} values recorded was the more sigmoidal character of the saturation curves. Thus, the A305F mutation resulted in a reduction in catalytic center accessibility for nifedipine and testosterone, whereas the A305S mutation resulted in changes in the autoactivation characteristics of the enzyme.

Table 4: Ketoconazole Inhibition Potency (K_i Values, μM) Measured against Various CYP3A4-Catalyzed Oxidation Reactions[a]

substrate	wild type	A305F	ratio to WT	A305S	ratio to WT
testosterone	0.043 ± 0.005	2.2 ± 0.3	51	0.021 ± 0.003	0.5
erythromycin	0.050 ± 0.014	0.55 ± 0.05	11	0.06 ± 0.02	1.2
nifedipine	0.05 ± 0.01	0.73 ± 0.24	15	0.03 ± 0.01	0.6

[a] Nifedipine oxidase and testosterone 6β-hydroxylase inhibition experiments were carried out with substrate concentrations equal to the S_{50} for each CYP3A4 enzyme form. Erythromycin *N*-demethylase inhibition experiments were carried out using 10 μM *N*-methyl[^{14}C]-erythromycin for all enzyme forms.

The apparent S_{50} values determined in this study are in good agreement with those published by other laboratories, for example, testosterone 6β-hydroxylase $S_{50} = 47$ μM (*28*), nifedipine oxidase $S_{50} = 15$ μM (*29*), and erythromycin $S_{50} = 18 - 57$ μM (*30*). However, the reaction conditions chosen for these studies resulted in turnover rates lower than those that have been reported in some experimental systems.

The character of the erythromycin *N*-demethylase saturation profiles were somewhat different from the other substrates that were studied (Figure 2). Here, all three enzyme forms displayed hyperbolic kinetics, with the least-active enzyme (A305F) saturated at the lowest erythromycin concentration and the activity of the most active enzyme (A305S) remaining incompletely saturated, even at 600 μM erythromycin. It appeared that the A305F mutation had increased the affinity of the CYP3A4 active site for erythromycin resulting in reduced catalytic activity, whereas the reverse had occurred with the A305S mutation.

The diazepam oxidation experiments were carried out with substrate concentrations up to 500 μM due to solubility limitations. This corresponded to 0−2 times the S_{50} concentration, which, as found by Ono et al. (*31*), yielded substrate saturation data that did not approach the V_{max} asymptote.

Table 5: Erythromycin *N*-Demethylase Inhibition Potencies (K_i Values, μM) of Various Azole-Containing Compounds[a]

inhibitor	wild type	A305F	ratio to WT	A305S	ratio to WT
ketoconazole	0.050 ± 0.014	0.55 ± 0.05	11	0.059 ± 0.015	1.2
clotrimazole	<0.03	0.27 ± 0.08	>9	<0.03	1.0
miconazole	0.05 ± 0.02	0.16 ± 0.02	3	0.07 ± 0.02	1.4
econazole	0.04 ± 0.01	0.6 ± 0.1	15	0.07 ± 0.02	1.8
1-phenylimidazole	2.7 ± 0.4	16 ± 2	6	4.8 ± 0.4	1.8
1-(2-trifluoromethyl)phenylimidazole	0.8 ± 0.1	13 ± 2	16	4.9 ± 0.6	6.1
1-(3,4-dichloro)phenylimidazole	2.1 ± 0.4	12 ± 4	6	3.0 ± 0.7	1.4

[a] All inhibition experiments were carried out using 10 μM *N*-methyl[^{14}C]erythromycin.

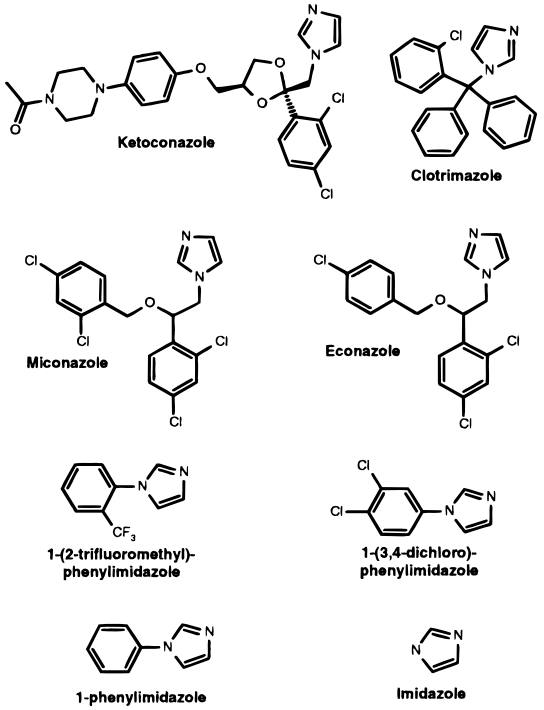

FIGURE 6: Chemical structures of azole-containg compounds used in this study.

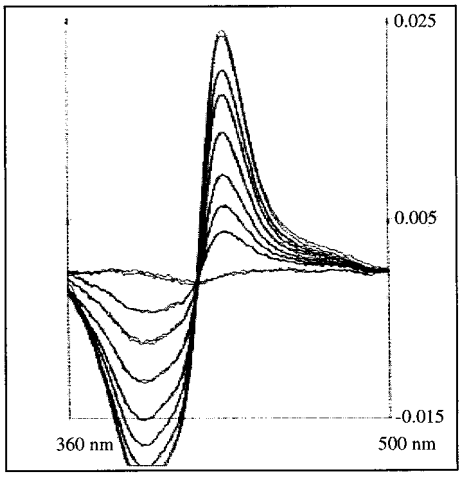

FIGURE 7: Use of difference spectroscopy to measure ketoconazole binding to CYP3A4. Overlaid difference traces of purified wild-type CYP3A4, recorded in duplicate, are shown with addition of 0.2 to 30 μM ketoconazole. Spectra were recorded between 500 and 360 nm with a range of −0.015 to 0.025 milliadsorption units. Growth of the 425 nm difference peak was used to assess percentage enzyme saturation.

Here, the difference between fitting a rectangular hyperbola or a sigmoid curve to the data had a large effect on the S_{50} and V_{max} values that were determined (Table 6). A sigmoidal curve gave a better fit to the data, with lower residuals and reduced estimated errors, especially in the low concentration

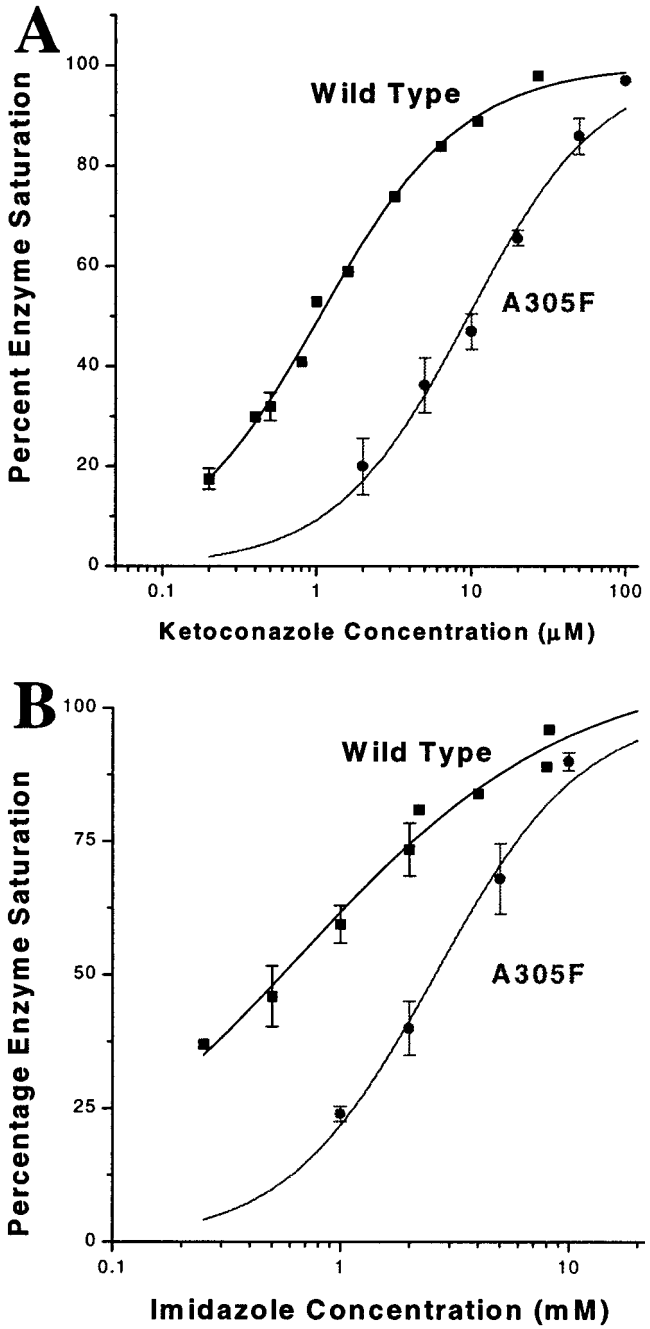

FIGURE 8: Binding of azole ligands to CYP3A4 measured by difference spectroscopy. Change in 425 nm absorption with ligand concentration plotted as a percentage of maximal (saturating) absorption change for (A) ketoconazole (μM) and (B) imidazole (mM). Sigmoidal curves have been fitted to the data. Wild-type data is denoted by filled squares, A305F data by filled circles.

Table 6: Comparison of Hyperbolic and Sigmoidal Substrate Saturation Curve Fits Using Diazepam 3-hydroxylase Activity as an Example[a]

CYP3A4 form	parameter	hyperbolic data fit	sigmoidal data fit
wild type	S_{50}	440 ± 140	180 ± 30
	V_{max}	3.9 ± 0.7	2.4 ± 0.3
	n		1.6 ± 0.3
A305S mutant	S_{50}	940 ± 460	210 ± 15
	V_{max}	4.1 ± 1.5	1.5 ± 0.1
	n		2.5 ± 0.4

[a] S_{50} units are μM, V_{max} units are pmol product/min/pmol P450. *n* is the Hill coefficient.

(<100 μM) range, but resulted in much lower V_{max} and S_{50} estimates.

The sensitivity of diazepam oxidase regioselectivity to the alanine 305 → serine mutation and abolition of diazepam oxidation activity by the A305F mutation suggested that diazepam binding in the active site of CYP3A4 occurred closer to the A305 region than the testosterone binding.

If a method to generate crystals of CYP3A4 were available, it would be interesting to determine whether this hypothesis is correct—that the sensitivity of a given CYP3A4 activity to the A305S and A305F mutations is dependent upon which part of the active site is most involved in substrate binding. These data also predict that nifedipine, whose metabolic activity is least diminished by the A305F mutation, was less intimately associated with the A305 region of the active site than diazepam or testosterone. The work of Domanski et al. (*3*) has shown that the α-naphthoflavone interaction characteristics of CYP3A4 were modified by the A305V mutation, suggesting that this region of the active site was also important for α-naphthoflavone binding. Further investigations will determine whether α-naphthoflavone can be used as an additional probe of the A305F and A305S mutation effects on the CYP3A4 active site.

Azole Probing of Active Site. Modification of the active-site environment by site-directed mutagenesis, which results in a change in binding affinity for some azole ligand structures but not others, is strong evidence for contact between the mutagenized region of the active site and features specific to the inhibitor. Active site modifications which affect the binding affinity of all azole inhibitors indicate the amino acid substitutions to affect accommodation of a feature common to all the inhibitors examined − the azole moiety itself.

Although this approach is useful for direct observations, the amount of enzyme required for accurate difference spectroscopy prevented K_d determinations of values lower than 0.5 μM. As the more potent azole inhibitors exhibited K_i values well below this concentration, a more sensitive assay system was required. In this study, the radiometric erythromycin *N*-demethylase assay has been used to determine the K_i values for the azole inhibitors that were studied.

Modification of CYP3A4 Inhibition Characteristics. The substrate metabolism data indicated that the A305S mutation altered the character of one region of the CYP3A4 active site, whereas the A305F mutation caused steric blocking of that active site region. How does the azole inhibition data fit such a hypothesis?

The inhibition experiments detailed in this study showed that the azole inhibitors tested were insensitive to the A305S mutation, suggesting that the hydrophobicity of the A305 active-site region was largely irrelevant to azole inhibitor binding. However, reduction of the active-site volume in this region had a very significant effect upon the azole compound inhibition potency. Clotrimazole, the most potent inhibitor studied, showed a >9-fold shift in K_i value as a result of the A305F mutation in the erythromycin *N*-demethylase inhibition assay. The K_i values for ketoconazole, econazole, and 1-(2-trifluoromethyl)phenylimidazole were increased more than 10-fold above the corresponding wild-type values. Surprisingly, the K_i values for miconazole and econazole were quite different in the A305F mutant. These two compounds differ only by the presence of a chlorine atom (Figure 6) and exhibited identical inhibition potencies toward both the wild type and the A305S mutant enzymes. An examination of miconazole derivatives may show whether the unexpectedly high inhibition potency of miconazole is part of a trend or an isolated result.

An enzyme modification that prevented the accommodation of large, hydrophobic inhibitors could do so by reducing the total enzyme active-site volume. The inhibition properties of small azole-containg compounds such as 1-phenylimidazole, whose inhibition constants were around 10-fold higher for the A305F mutant than for either the wild type or the A305S mutant, showed that the A305F mutation affected accommodation of the azole moiety at the catalytic center. Unlike ketoconazole or clotrimazole, in which a change in one of many amino acid−ligand interactions could alter the binding affinity, small azole inhibitors do not make sufficient contacts in the extensive CYP3A4 active site for anything other than steric blocking of the catalytic center to reduce ligand-binding affinity.

A final demonstration that the A305F mutation results in reduced azole inhibition potency was obtained using the smallest available azole inhibitor, imidazole, in the direct binding spectroscopic assay. As seen with ketoconazole, a far higher imidazole concentration was required to saturate the A305F mutant to the same extent as the wild type. Thus, the A305F mutation affected a ligand molecule placed very close to the heme iron. The reduction in imidazole binding strength indicated that the affinity of the A305F enzyme active site for binding of the *azole moiety itself* was reduced, causing a general, rather than ligand-specific, reduction in azole containing inhibitor affinities.

CONCLUSIONS

This study has demonstrated that the A305F mutation dramatically reduces the CYP3A4 inhibition potency of ketoconazole and other azole-containing compounds, while retaining metabolic activity toward nifedipine, erythromycin, and testosterone. The reduction of ketoconazole inhibition potency was independent of the substrate oxidation assay system, as similar K_i values were generated for each enzyme form using three very different substrates for the enzyme activity assays. The reduction of heme binding affinity was confirmed as the physical basis of inhibition potency reduction by direct spectroscopic observation, an experiment in which competition for the active site with a substrate was not an issue. Moreover, these studies have shown that this reduction in binding affinity was a result of the A305F mutation and appeared to be a phenomenon common to

azole-containing compounds, varying from the most potent inhibitor clotrimazole to the least potent, imidazole.

Extension of the amino acid 305 side chain appeared to have caused partial steric blocking of the catalytic center close to the heme. This region of the active site has been shown to be universally important for the binding of azole-containing heme ligands. These studies have also demonstrated that it was critical to the binding and oxidation of some CYP3A4 substrates, such as diazepam, but far less important to others, such as nifedipine. The results of this study have been explained in terms of an inflexible enzyme model and partial steric blocking of the active site. As in all cytochrome P450 mutagenesis studies, it is important to consider the possible effects of the mutation upon the overall enzyme structure and enzyme−substrate interactions. The crystallography work of Poulos and Howard (*32*) on $P450_{cam}$ has shown that the I-helix can move to accommodate azole heme ligands. The effect of alanine 305 mutagenesis on I-helix mobility and the distance the helix would have to be displaced to accommodate a ligand are other factors that could help to explain our findings.

Our findings have demonstrated the molecular-model prediction that alanine 305 made some substrate contacts in a region of the CYP3A4 active site close to the catalytic center. Further metabolic studies are being carried out to examine the effects of these A305 mutations on the auto-activation and allosteric activation characteristics of CYP3A4. The results of this study add to our knowledge of CYP3A4 structure−function relationships, which will increase the quality of active site model-building studies in the future.

REFERENCES

1. Li, A. P., Kaminski, D. L., and Rasmussen, A. (1995) *Toxicology 104*, 1−8.
2. Singer, M. I., Shapiro, L. E., and Shear, N. H. (1997) *J. Am. Acad. Derm. 37*, 765−771.
3. Domanski, T. L., Liu, J., Harlow, G. R., and Halpert, J. R. (1998) *Arch. Biochem. Biophys. 350*, 223−232.
4. Harlow, G. R., and Halpert, J. R. (1997) *J. Biol. Chem. 272*, 5396−5402.
5. He, Y. A., He, Y. Q., Szklarz, G. D., and Halpert, J. R. (1997) *Biochemistry 36*, 8831−8839.
6. Poulos, T. L. (1995) *Curr. Opin. Struct. Biol. 5*, 767−774.
7. Nelson, D. R., and Strobel, H. W. (1989) *Biochemistry 28*, 656−660.
8. Gerber, N. C., and Sligar, S. G. (1992) *J. Am. Chem. Soc. 114*, 8742−8743.
9. Gerber, N. C., and Sligar, S. G. (1994) *J. Biol. Chem. 269*, 4260−4266.
10. Raag, R., Martinis, S. A., Sligar, S. G., and Poulos, T. L. (1991) *Biochemistry 30*, 11420−11429.
11. Yeom, H., and Sligar, S. G. (1997) *Arch. Biochem. Biophys. 337*, 209−216.
12. Vidakovic, M., Sligar, S. G., Li, H., and Poulos, T. L. (1998) *Biochemistry 37*, 9211−9219.
13. Koymans, L. M., Vermeulen, N. P., Baarslag, A., and Donne-Op den Kelder, G. M. (1993) *J. Comput.-Aided Mol. Des. 7*, 281−289.
14. Modi, S., Paine, M. J., Sutcliffe, M. J., Lian, L. Y., Primrose, W. U., Wolf, C. R., and Roberts, G. C. (1996) *Biochemistry 35*, 4540−4550.
15. Ellis, S. W., Hayhurst, G. P., Smith, G., Lightfoot, T., Wong, M. M., Simula, A. P., Ackland, M. J., Sternberg, M. J., Lennard, M. S., and Tucker, G. T. (1995) *J.f Biol. Chem. 270*, 29055−29058.
16. Szklarz, G. D., and Halpert, J. R. (1997) *J. Comput.-Aided Mol. Des. 11*, 265−272.
17. Ervine, C. M., Matthew, D. E., Brennan, B., and Houston, J. B. (1996) *Drug Metab. Dispos. 24*, 211−215.
18. Maurice, M., Pichard, L., Daujat, M., Fabre, I., Joyeux, H., Domergue, J., and Maurel, P. (1992) *FASEB J. 6*, 752−758.
19. von Moltke, L. L., Greenblatt, D. J., Duan, S. X., Harmatz, J. S., Wright, C. E., and Shader, R. I. (1996) *J. Clin. Psychopharmacol. 16*, 104−112.
20. Baldwin, S. J., Bloomer, J. C., Smith, G. J., Ayrton, A. D., Clarke, S. E., and Chenery, R. J. (1995) *Xenobiotica 25*, 261−270.
21. Blake, J. A., Pritchard, M., Ding, S., Smith, G. C., Burchell, B., Wolf, C. R., and Friedberg, T. (1996) *FEBS Lett. 397*, 210−214.
22. Pritchard, M. P., Ossetian, R., Li, D. N., Henderson, C. J., Burchell, B., Wolf, C. R., and Friedberg, T. (1997) *Arch. Biochem. Biophys. 345*, 342−354.
23. Pritchard, M. P., Glancey, M. J., Blake, J. A., Gilham, D. E., Burchell, B., Wolf, C. R., and Friedberg, T. (1998) *Pharmacogenetics 8*, 33−42.
24. Vermilion, J. L., and Coon, M. J. (1974) *Biochem. Biophys. Res. Commun. 60*, 1315−1322.
25. Kunkel, T. A. (1985) *Proc. Natl. Acad. Sci. U.S.A. 82*, 488−492.
26. Moody, G. C., Griffin, S. J., Mather, A. N., McGinnity, D. F., and Riley, R. J. (1999) *Xenobiotica 29*, 53−75.
27. Dawson, J. H., Andersson, L. A., and Sono, M. (1982) *J. Biol. Chem. 257*, 3606−3617.
28. Waxman, D. J., Lapenson, D. P., Aoyama, T., Gelboin, H. V., Gonzalez, F. J., and Korzekwa, K. (1991) *Arch. Biochem. Biophys. 290*, 160−166.
29. Ingelman-Sundberg, M., Hagbjork, A. L., Ueng, YF, Yamazaki, H., and Guengerich, F. P. (1996) *Biochem. Biophys. Res. Commun. 221*, 318−322.
30. McGinnity, D. F., Griffin, S. J., Moody, G. C., Voice, M., Hanlon, S., Friedberg, T., and Riley, R. J. (1999) *Drug Metab. Dispos.* (in press).
31. Ono, S., Hatanaka, T., Miyazawa, S., Tsutsui, M., Aoyama, T., Gonzalez, F. J., and Satoh (1996) *Xenobiotica 26*, 1155−1166.
32. Poulos, T. L., and Howard, A. J. (1987) *Biochemistry 26*, 8165−8174.

BI992372U